Inorg. Chem. **2008**, *47*, 9182−9192

Metal−Metal Communication in Copper(II) Complexes of Cyclotetraphosphazene Ligands

Eric W. Ainscough,*,† Andrew M. Brodie,*,† Ross J. Davidson,† Boujemaa Moubaraki,‡ Keith S. Murray,‡ Carl A. Otter,† and Mark R. Waterland†

Chemistry-Institute of Fundamental Sciences, Massey University, Private Bag 11 222, Palmerston North, New Zealand 4442, and School of Chemistry, Building 23, Monash University, Clayton, Victoria 3800, Australia

Received May 14, 2008

Copper(II) chloride and bromide react with the pyridyloxy-substituted cyclotetraphosphazene ligands, octakis(2-pyridyloxy)cyclotetraphosphazene (L^1), and octakis(4-methyl-2-pyridyloxy)cyclotetraphosphazene (L^2), to form the dimetallic complexes, $[L(CuX_2)_2]$ (L = L^1, X = Br; L = L^2, X = Cl or Br), and $[\{L^1(CuCl_2)_2\}_n]$. Single crystal X-ray crystallography shows the complex $[\{L^1(CuCl_2)_2\}_n]$ to be a coordination polymer propagated by interligand "Cu(μ-Cl)$_2$Cu" bridges whereas $[L^2(CuCl_2)_2]$ forms discrete dimetallic cyclotetraphosphazene-based moieties. The variable temperature magnetic susceptibility data for $[\{L^1(CuCl_2)_2\}_n]$ are consistent with a weak antiferromagnetic exchange interaction between the copper(II) centers occurring via the bridging chloride ions. $[L^2(CuCl_2)_2]$ and $[L(CuBr_2)_2]$ (L = L^1 and L^2) exhibit normal Curie-like susceptibilities. The abstraction of a chloride ion, using $[Ag(MeCN)_4](PF_6)$, from each copper site in $[L^2(CuCl_2)_2]$, affords the new complex, $[L^2(CuCl)_2](PF_6)_2$, in which the two copper(II) ions are separated by "N—P═N—P═N" phosphazene bridges. Electron spin resonance and variable temperature magnetic measurements indicate the occurrence of weak antiferromagnetic coupling between the unpaired electrons on the copper(II) centers. Density Functional Theory (DFT) calculations on the $[L^2(CuCl)_2]^{2+}$ dication and the related cyclotriphosphazene complex, $[L^4(CuCl_2)_2]$ (L^4 = hexakis(4-methyl-2-pyridyloxy)cyclotriphosphazene), have identified "electron-density-bridge" molecular orbitals which involve Cu 3d orbitals overlapping with the non-bonding N-based molecular orbitals on the phosphazene rings as the pathway for this interaction.

Introduction

The metal-binding properties of substituted cyclic and linear polyphosphazene systems (Chart 1) continue to attract interest and have been the subject of several recent reviews.[1−3] The facile substitution chemistry of the chloropolyphosphazene precursors enables the phosphazene scaffolds to be readily modified with a variety of different pendant ligand types. A desirable goal is the preparation of polymeric phosphazenes that are loaded with metal-ions that can communicate through ligand bridges, thus giving rise to polymers with interesting magnetic or conducting properties.

Chart 1

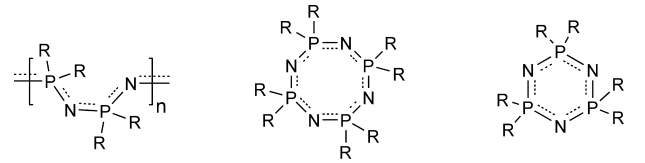

The cyclic systems are used as models for the high molecular weight polymers and by far the most extensively studied are the derivatives of cyclotriphosphazene. For example, we and others[4−9] have explored the multimodal coordination abilities of the fully substituted ligands hexakis(2-pyridyloxy)cyclotriphosphazene (L^3) and hexakis(4-methyl-2-pyridyloxy)cyclotriphosphazene (L^4) (Chart 1). However,

* To whom correspondence should be addressed. E-mail: e.ainscough@massey.ac.nz (E.W.A.), a.brodie@massey.ac.nz (A.M.B.).
† Massey University.
‡ Monash University.

(1) *Applicative Aspects of Cyclophosphazenes*; Gleria, M., De Jaeger, R., Eds.; Nova Science Publishers, Inc.: New York, 2004.
(2) Chandrasekhar, V.; Thilagar, P.; Murugesa Pandian, B. *Coord. Chem. Rev.* **2007**, *259*, 1045–1074.
(3) Pertici, P.; Vitulli, G.; Gleria, M.; Facchin, G.; Milani, R.; Bertani, R. *Macromol. Symp.* **2006**, *235*, 98–114.

10.1021/ic8008706 CCC: $40.75
Published on Web 09/26/2008

it is arguable that the cyclic tetramers are better models for the polymer because of the greater flexibility of the eight-membered phosphazene ring.[10a] For this reason, we have embarked on a study of such systems and have recently reported the synthesis and characterization of a series of pyridyloxy-substituted 2,2′-dioxybiphenylcyclotetraphosphazene metal halide complexes.[10b] Other cyclotetraphosphazene complexes, for which X-ray structural data is reported, include metallocene,[11−14] tungsten tetracarbonyl,[15] and platinum dichloride[16−18] complexes. Data also exist for protonated cationic cyclotetraphosphazenes, which can act as an ion pair for complex anions[16,19,20] or as cationic ligands.[21]

Since complexes that contain a neutral cyclotetraphosphazene acting as a bridging ligand by binding through the phosphazene ring nitrogen atoms are not known, our first task was to attempt to synthesize such molecules, followed by a study of the ability of such inorganic ring systems, which have limited P−N multiple bonding capacity, to communicate electronic information between the metal centers. Unlike carbon-based, π-conjugated systems, ab initio calculations show the P−N multiple bonding character of linear and cyclic phosphazenes can be rationalized in terms of negative hyperconjugation and ionic bonding, with the latter being the dominant feature.[22] A comparison of metal−metal interactions via conjugated organic systems would clearly be of interest.

We recently reported the syntheses and crystal structures of the ligands octakis(2-pyridyloxy)cyclotetraphosphazene (L^1) and octakis(4-methyl-2-pyridylxy)cyclotetraphosphazene (L^2) (Chart 1).[23] These cyclotetraphosphazene ligands have the potential to bind many metal ions, but this has not been extensively examined and thus they may provide models for metal-rich polyphosphazenes as well. Structural diversity would be expected because of the ability of these molecules to bind metal ions through the phosphazene ring nitrogen atoms and, as well, the pyridyloxy pendant arms may coordinate in a myriad of modes similar to that reported for analogous cyclotriphosphazenes. Indeed a comparison of the coordination chemistry of L^1 and L^2 with the trimeric analogues[4−9] would be of value. Here we have studied the reactions of L^1 and L^2 with copper(II) halides and find that only the 2:1 products are formed when 1 or 2 equiv of the metal salt are added. Reported are the crystal structures of the first dinuclear complexes containing a bridging cyclotetraphosphazene, these being $[\{L^1(CuCl_2)_2\}_n]$, $[L^2(CuCl_2)_2]$, and $[L^2(CuCl)_2](PF_6)_2$. $[\{L^1(CuCl_2)_2\}_n]$ is a coordination polymer propagated by interligand "Cu(μ-Cl)$_2$Cu" bridges. This complex and $[L^2(CuCl_2)_2]$ (where each copper has an "N_2Cl_2" donor set using nitrogen atoms from pyridine groups on non-geminal phosphorus atoms) both exhibit a previously unseen coordination mode for cyclotetraphosphazene ligands. In these complexes one of the chloride ligands successfully competes with the weakly basic phosphazene ring nitrogen atom for the copper sites. $[L^2(CuCl)_2](PF_6)_2$ is the product of the reaction between $[L^2(CuCl_2)_2]$ and $[Ag(MeCN)_4](PF_6)$ (Scheme 1). Upon the removal of one chloride ion per copper site two of the free pyridine ring nitrogen donors swing in to bind to the copper thus encouraging a phosphazene ring nitrogen to also bind, and in so doing the system behaves as a κ^5 *bis*-tetrapodal bridging ligand. Each copper has a "N_5Cl" donor set. Thus, three new bridging modes for cyclotetraphosphazenes have been established, and their nature has been probed by electron spin resonance (ESR) and variable temperature magnetic data for the complexes $[\{L^1(CuCl_2)_2\}_n]$, $[L^2(CuCl_2)_2]$, and their bromo analogues, as well as $[L^2(CuCl)_2](PF_6)_2$. For the latter compound, the results suggest weak antiferromagnetic coupling between the copper(II) centers and, to help understand the mechanism of this unexpected interaction, Density Functional Theory (DFT) calculations have been carried out. As far as we are aware, this complex and its trimeric analogue, $[L^4(CuCl_2)_2]$ (Chart 2)[4b] are the only ones known where two magnetically coupled paramagnetic metal ions are bound directly to the phosphazene ring nitrogen atoms, and hence they offer a unique opportunity to probe the nature of the P−N bond in phosphazenes.

Experimental Section

General Information. Analytical grade solvents were used without further purification. $CuCl_2 \cdot 2H_2O$ was dehydrated at 140 °C before use, and $[Ag(MeCN)_4]PF_6$ was prepared using the method

(4) (a) Ainscough, E. W.; Brodie, A. M.; Depree, C. V. *J. Chem. Soc., Dalton Trans.* **1999**, 4123–4124. (b) Ainscough, E. W.; Brodie, A. M.; Depree, C. V.; Moubaraki, B.; Murray, K. S.; Otter, C. A. *Dalton Trans.* **2005**, 3337–3343.
(5) Ainscough, E. W.; Brodie, A. M.; Depree, C. V.; Jameson, G. B.; Otter, C. A. *Inorg. Chem.* **2005**, *44*, 7325–7327.
(6) Ainscough, E. W.; Brodie, A. M.; Depree, C. V.; Otter, C. A. *Polyhedron* **2006**, *25*, 2341–2352.
(7) Ainscough, E. W.; Brodie, A. M.; Davidson, R. J.; Otter, C. A. *Inorg. Chem. Commun.* **2008**, *11*, 171–174.
(8) Chandrasekhar, V.; Pandian, B. M.; Azhakar, R. *Inorg. Chem.* **2006**, *45*, 3510–3518.
(9) Chandrasekhar, V.; Pandian, B. M.; Azhakar, R. *Polyhedron* **2008**, *27*, 255–262.
(10) (a) Ainscough, E. W.; Brodie, A. M.; Chaplin, A. B.; Derwahl, A.; Harrison, J. A.; Otter, C. A. *Inorg. Chem.* **2007**, *46*, 2575–2583. (b) Ainscough, E. W.; Brodie, A. M.; Derwahl, A.; Kirk, S.; Otter, C. A. *Inorg. Chem.* **2007**, *46*, 9841–9852.
(11) Herberhold, M.; Hofmann, A.; Milius, W. *Z. Anorg. Allg. Chem.* **1997**, *623*, 1599–1608.
(12) Herberhold, M.; Hoffmann, A.; Milius, W. *Z. Anorg. Allg. Chem.* **1997**, *623*, 545–553.
(13) Allcock, H. R.; Lavin, K. D.; Riding, G. R.; Whittle, R. R. *Organometallics* **1984**, *3*, 663–669.
(14) Allcock, H. R.; Lavin, K. D.; Riding, G. R.; Suszko, P. R.; Whittle, R. R. *J. Am. Chem. Soc.* **1984**, *106*, 2337–2347.
(15) Calhoun, H. P.; Paddock, N. L.; Trotter, J. *J. Chem. Soc., Dalton Trans.* **1973**, 2708–2712.
(16) O'Brien, J. P.; Allen, R. W.; Allcock, H. R. *Inorg. Chem.* **1979**, *18*, 2230–2235.
(17) O'Brien, J. P.; Allen, R. W.; Allcock, H. R. *J. Am. Chem. Soc.* **1977**, *99*, 3987–3991.
(18) Allcock, H. R.; Allen, R. W.; O'Brien, J. P. *Chem. Commun.* **1976**, 717–718.
(19) Calhoun, H. P.; Trotter, J. *J. Chem. Soc., Dalton Trans.* **1974**, 377–381.
(20) Trotter, J.; Whitlow, S. H. *J. Chem. Soc. A* **1970**, 460–464.
(21) Trotter, J.; Whitlow, S. H. *J. Chem. Soc. A* **1970**, 455–459.
(22) Chaplin, A. B.; Harrison, J. A.; Dyson, P. J. *Inorg. Chem.* **2005**, *44*, 8407–8417.
(23) Ainscough, E. W.; Brodie, A. M.; Derwahl, A. *Polyhedron* **2003**, *22*, 189–197.

Scheme 1

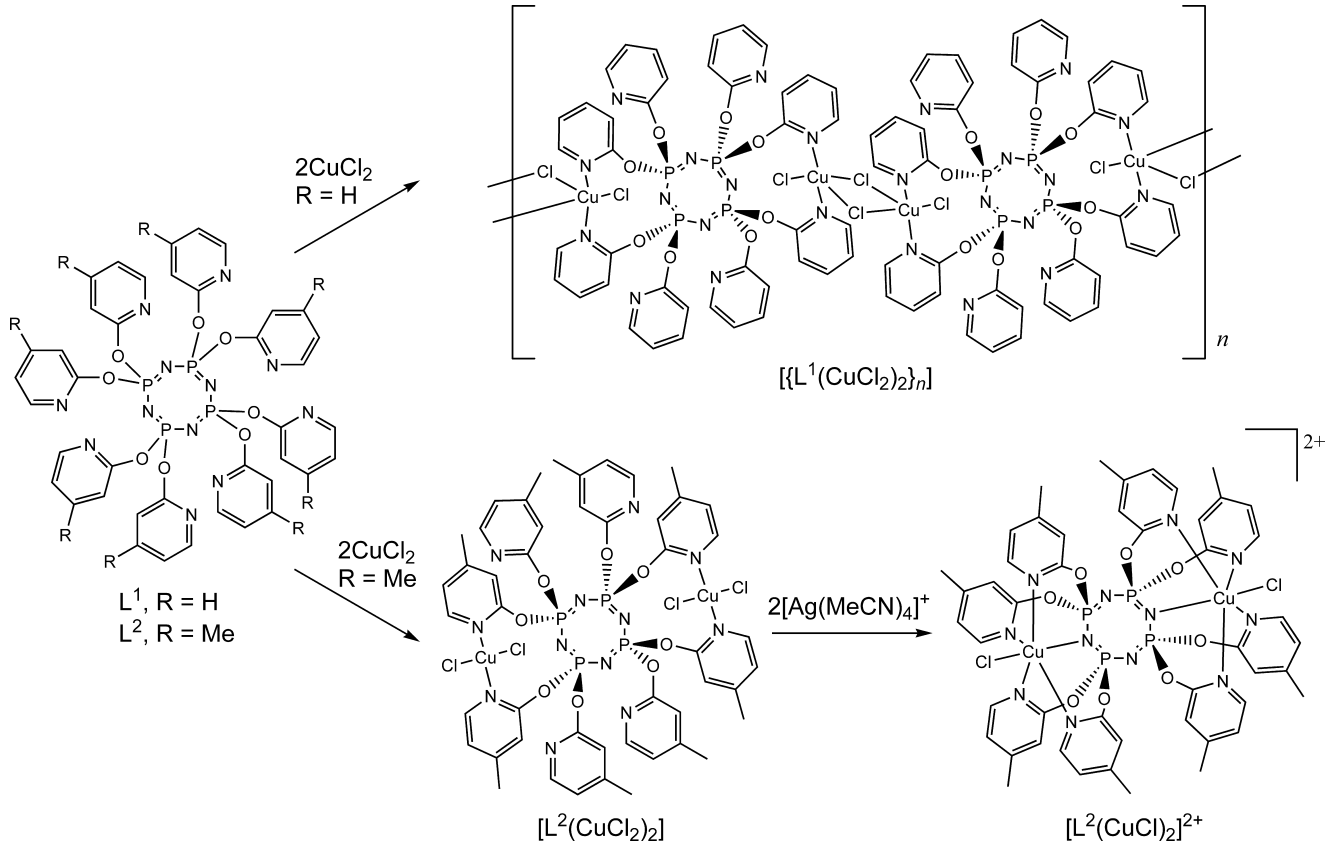

Chart 2

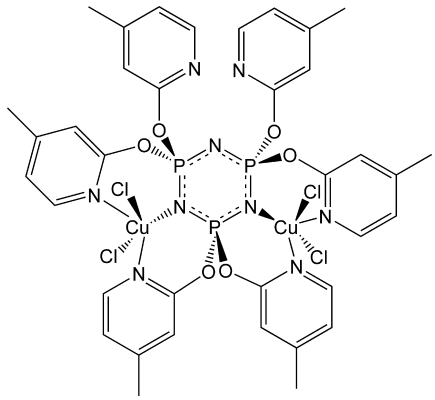

described for the analogous copper(I) complex.[24] The ligands L^1 and L^2 were prepared as previously described.[23] Microanalyses were performed by the Campbell Microanalytical Laboratory, University of Otago. IR spectra were run as KBr discs on a Perkin-Elmer FT-IR Paragon 1000 spectrometer, and electronic absorption spectra were recorded using a Shimadzu UV-310−310PC scanning spectrometer. Electrospray mass spectra were obtained from CH_3CN solutions on a Micromass ZMD spectrometer run in positive ion mode. Listed peaks correspond to the most abundant isotopomer; assignments were made by a comparison of observed and simulated spectra. EPR spectra were recorded at 110 K on a Varian E-104A spectrometer equipped with a E-257 variable-temperature controller and operating at about 9.0 GHz. The spectral *g* values were calibrated with (diphenylpicryl)hydrazyl (DPPH) as a standard. Room temperature magnetic susceptibilities were measured by the Faraday method on a Cahn model 7550 Millibalance. A Quantum Design Squid magnetometer was used for the variable temperature magnetic susceptibility measurements (4.2−300 K). A 30 mg sample of the complex was contained in a gel capsule that was held in a drinking straw attached to the end of the sample rod. A direct current field of 1 T was employed. The non-linear least-squares fitting program used to fit the data was an in-house program.

Complex Syntheses. [{L^1($CuCl_2$)$_2$}$_n$]. To a solution of L^1 (0.093 g, 0.10 mmol) in CH_2Cl_2 (10 mL) was added $CuCl_2$ (0.025 g, 0.19 mmol), and the mixture was stirred at room temperature overnight during which time a pale blue precipitate developed. The precipitate was collected by filtration and recrystallized from hot MeCN to give a crop of feathery, pale blue crystals that was dried under vacuum. Yield: 0.060 g (49%). Anal. Required for $C_{40}H_{32}Cl_4Cu_2N_{12}O_8P_4$: C, 39.98; H, 2.68; N, 13.99%. Found: C, 39.35; H, 2.92; N, 13.78%. ESMS: *m*/*z* 1030 $[L^1CuCl]^+$, 995 $[L^1Cu]^+$. IR υ_{PN} (cm^{-1}): 1239, 1203.

[L^1($CuBr_2$)$_2$]. To a solution of L^1 (0.093 g, 0.10 mmol) in CH_2Cl_2 (10 mL) was added $CuBr_2 \cdot H_2O$ (0.041 g, 0.17 mmol), and the mixture was stirred at room temperature overnight, during which time a green precipitate developed. The precipitate was collected by filtration, recrystallized from hot MeCN, and dried under vacuum. Yield: 0.065 g, (47%). Anal. Required for $C_{40}H_{32}Br_4Cu_2N_{12}O_8P_4$: C, 34.83; H, 2.34; N, 12.19%. Found: C, 34.99; H, 2.44; N, 12.23%. ESMS: *m*/*z* 1074 $[L^1CuBr]^+$, 995 $[L^1Cu]^+$. IR υ_{PN} (cm^{-1}): 1231, 1203.

[L^2($CuCl_2$)$_2$]. To a solution of L^2 (0.104 g, 0.10 mmol) in CH_2Cl_2 (10 mL) was added $CuCl_2$ (0.025 g, 0.19 mmol), and the mixture was stirred at room temperature overnight to give a green solution. The solution was filtered and taken to dryness on a rotary

(24) Kubas, G. J. *Inorg. Synth.* **1990**, *28*, 68–70.

Table 1. Crystal and Refinement Data for All Complexes

	$[\{L^1(CuCl_2)_2\}\cdot 2MeCN\cdot H_2O]_n$	$[L^2(CuCl_2)_2]$	$[L^2(CuCl)_2](PF_6)_2\cdot 6MeCN$
empirical formula	$C_{44}H_{40}Cl_4Cu_2N_{14}O_9P_4$	$C_{48}H_{48}Cl_4Cu_2N_{12}O_8P_4$	$C_{60}H_{66}Cl_2Cu_2F_{12}N_{18}O_8P_6$
M	1301.68	1313.74	1779.11
T (K)	89(2)	87(2)	87(2)
crystal system	orthorhombic	monoclinic	triclinic
space group	*Pnnm*	*P*2(1)/*n*	$P\bar{1}$
a (Å)	12.2330(13)	14.29530(10)	11.3206(2)
b (Å)	14.5403(16)	10.5046(2)	14.3026(3)
c (Å)	15.9717(16)	18.2248(3)	14.6652(5)
α (deg)	90	90	103.172(2)
β (deg)	90	92.204(1)	108.032(2)
γ (deg)	90	90	110.8230(10)
V (Å^3)	2840.9(5)	2734.73(7)	1951.91(9)
Z	2	2	1
μ(Mo Kα) (mm^{-1})	1.113	1.115	0.827
ρ_{calc} (g cm^{-3})	1.521	1.595	1.514
2θ max (deg)	50.70	52.78	50.70
no. of unique reflections	2649	5583	7383
data/restraints/parameters	2649/64/222	5583/0/356	7383/69/537
final R indices [$I > 2\sigma(I)$]	$R_1 = 0.0469$, $wR_2 = 0.1310$	$R_1 = 0.0318$, $wR_2 = 0.0658$	$R_1 = 0.0415$, $wR_2 = 0.1051$
R indices (all data)	$R_1 = 0.0647$ $wR_2 = 0.1408$	$R_1 = 0.0404$ $wR_2 = 0.0694$	$R_1 = 0.0543$ $wR_2 = 0.1128$
goodness of fit on F^2	1.122	1.085	0.994

evaporator. The residue was dissolved in MeCN, and Et_2O vapor was allowed to diffuse into the solution to give a crop of blue crystals that was dried under vacuum. Yield: 0.100 g (76%). Anal. Required for $C_{48}H_{48}Cl_4Cu_2N_{12}O_8P_4$: C, 43.88; H, 3.68; N, 12.79%. Found: C, 43.98; H, 3.75; N, 12.67%. ESMS: *m*/*z* 1142 $[L^2CuCl]^+$, 1107 $[L^2Cu]^+$. IR υ_{PN} (cm^{-1}): 1270, 1254, 1244.

$[L^2(CuBr_2)_2]$. To a solution of L^2 (0.104 g, 0.10 mmol) in CH_2Cl_2 (10 mL) was added $CuBr_2\cdot H_2O$ (0.041 g, 0.17 mmol), and the mixture was stirred at room temperature overnight to give a green solution. The solution was filtered and taken to dryness on a rotary evaporator. The residue was dissolved in hot MeCN and placed in a freezer to give a green precipitate that was collected by filtration and dried under vacuum. Yield: 0.050 g (33%). Anal. Required for $C_{48}H_{48}Cl_4Cu_2N_{12}O_8P_4$: C, 38.65; H, 3.24; N, 11.27%. Found: C, 38.94; H, 3.22; N, 11.24%. ESMS: 1188 $[L^2CuBr]^+$, 1107 $[L^2Cu]^+$. IR υ_{PN} (cm^{-1}): 1270, 1251, 1245.

$[L^2(CuCl)_2](PF_6)_2$. To a solution of L^2 (0.104 g, 0.10 mmol) in CH_2Cl_2 (15 mL) was added $CuCl_2$ (0.027 g, 0.20 mmol). The solution was stirred at room temperature over 2 h to give a green solution. A solution of $[Ag(MeCN)_4]PF_6$ (0.083 g, 0.20 mmol) in CH_2Cl_2 (5 mL) was added, and the mixture was allowed to stir overnight. The precipitate that formed was collected by filtration, and the filtrate discarded. The collected solid material was washed with MeCN, and the washings were collected and taken to dryness on a rotary evaporator. A pale blue crystalline material was obtained by vapor diffusion of Et_2O into a MeCN solution of the residue. Yield: 0.080 g (52%). Anal. Required for $C_{48}H_{48}Cl_2Cu_2F_{12}N_{12}O_8P_6$: C, 37.61; H, 3.16; N, 10.97%. Found: C, 37.45; H, 3.30; N, 10.78%. ESMS: *m*/*z* 1142 $[L^2CuCl]^+$, 1107 $[L^2Cu\}]^+$. IR υ_{PN} (cm^{-1}): 1294, 1278, 1242, 1213.

Crystallography. The X-ray data were collected on a Siemens P4 four circle diffractometer, using a Siemens SMART 1K CCD area detector. The crystals were mounted in an inert oil and irradiated with graphite monochromated Mo Kα ($\lambda = 0.71073$ Å) X-rays. The data were collected by the SMART program and processed with SAINT to apply Lorentz and polarization corrections to the diffraction spots (integrated three dimensionally). Crystal data are given in Table 1. The structures were solved by direct methods and refined using the SHELXTL program.[25] Hydrogen atoms were calculated at ideal positions. Two molecules of MeCN and one of H_2O per unit were identified in the structure of $[\{L^1(CuCl_2)_2\}_n]$. In the complex $[L^2(CuCl)_2](PF_6)_2$, which contains six molecules of MeCN per formula unit, pyridyloxy ring 2 shows disorder and was modeled in two slightly different orientations with occupancies of about 7:3. In the model, the nitrogen atoms from each part were given equivalent *x*, *y*, and *z* parameters.

Computational Details. Geometry optimizations were performed using the Gaussian 03 suite of programs[26a] using DFT at the B3LYP level with a 6−31G(d) basis set for all atoms. The optimizations were validated by comparisons of the P−N and phosphazene ring nitrogen to metal bond distances with the data obtained from the X-ray structures (see Figure S1, Supporting Information). As expected for DFT calculations, the bond lengths were overestimated although the differences were less than 2% for all bonds. Illustrations were created using GaussView 3.0.[26b]

Results and Discussion

We initially attempted to prepare complexes of 1:1 stoichiometry from the reaction of one molar equivalent of

(25) Sheldrick, G. M. *SHELXL Suite of Programs for Crystal Structure Analysis*; Institüt für Anorganische Chemie der Universität Göttingen: Göttingen, Germany, 1998.

(26) (a) Frisch, M. J.; Trucks, G. W.; Schlegel, H. B.; Scuseria, G. E.; Robb, M. A.; Cheeseman, J. R.; Montgomery, J. A., Jr.; Vreven, T.; Kudin, K. N.; Burant, J. C.; Millam, J. M.; Iyengar, S. S.; Tomasi, J.; Barone, V.; Mennucci, B.; Cossi, M.; Scalmani, G.; Rega, N.; Petersson, G. A.; Nakatsuji, H.; Hada, M.; Ehara, M.; Toyota, K.; Fukuda, R.; Hasegawa, J.; Ishida, M.; Nakajima, T.; Honda, Y.; Kitao, O.; Nakai, H.; Klene, M.; Li, X.; Knox, J. E.; Hratchian, H. P.; Cross, J. B.; Bakken, V.; Adamo, C.; Jaramillo, J.; Gomperts, R.; Stratmann, R. E.; Yazyev, O.; Austin, A. J.; Cammi, R.; Pomelli, C.; Ochterski, J. W.; Ayala, P. Y.; Morokuma, K.; Voth, G. A.; Salvador, P.; Dannenberg, J. J.; Zakrzewski, V. G.; Dapprich, S.; Daniels, A. D.;. Strain, M. C.; Farkas, O.; Malick, D. K.; Rabuck, A. D.; Raghavachari, K.; Foresman, J. B.; Ortiz, J. V.; Cui, Q.; Baboul, A. G.; Clifford, S.; Cioslowski, J.; Stefanov, B. B.; Liu, G.; Liashenko, A.; Piskorz, P.; Komaromi, I.; Martin, R. L.; Fox, D. J.; Keith, T.; Al-Laham, M. A.; Peng, C. Y.; Nanayakkara, A.; Challacombe, M.; Gill, P. M. W.; Johnson, B.; Chen, W.; Wong, M. W.; Gonzalez, C.; Pople, J. A. *Gaussian 03*, Revision D.01; Gaussian, Inc.: Wallingford, CT, 2004. (b) Dennington II, R.; Keith, T.; Millam, J.; Eppinnett, K.; Hovell, W. L.; Gilliland, R. *GaussView*, Version 3.0; Semichem, Inc.: Shawnee Mission, KS, 2003.

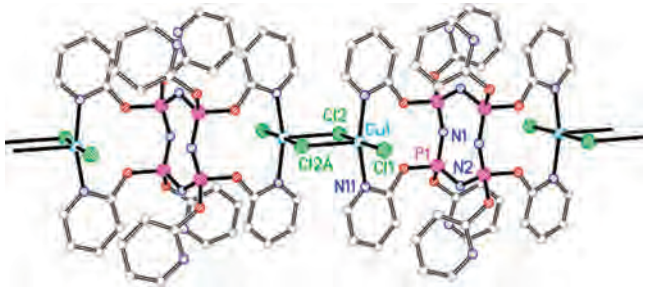

Figure 1. Part of the polymeric chain in $[\{L^1(CuCl_2)_2\}_n]$ with hydrogen atoms removed for clarity.

$CuCl_2$ with L^1 but it became apparent that the major product from the reaction was a complex of 2:1 stoichiometry. Hence, the reactions between L^1 or L^2 with two molar equivalents of $CuCl_2$ or $CuBr_2 \cdot H_2O$ were performed to produce the corresponding complexes of 2:1 stoichiometry. The complexes were isolated by recrystallization from MeCN, which initially produced deep yellow solutions for the complexes with chloride ligands. Analytically pure samples of the blue (chloro-substituted) or green (bromo-substituted) complexes consistent with the 2:1 formulation were obtained in yields ranging between 33 and 76%. Data presented in the following sections show that the complex of L^1 with $CuCl_2$ has a polymeric structure, that is, $[\{L^1(CuCl_2)_2\}_n]$, whereas the remaining copper halide complexes are dimetallic monomers with the formulation $[L(CuX_2)_2]$ ($L = L^1$, $X = Br$; $L = L^2$, $X = Cl$ or Br). When $[L^2(CuCl_2)_2]$ is treated with $[Ag(MeCN)_4]PF_6$, two chloride ions are abstracted and a new complex of stoichiometry $[L^2(CuCl)_2](PF_6)_2$ is obtained (Scheme 1).

Electrospray mass spectra (see Experimental Section) for the complexes were obtained from MeCN solutions, and these are all similar, showing *m*/*z* peaks for the ions $[LCuX]^+$ and $[LCu]^+$ ($L = L^1$ or L^2, $X = Cl$ or Br). No peaks assignable to dimetallic species were observed. Infrared P−N stretching frequencies can be assigned to strong split bands observed in the 1294 to 1203 cm^{-1} region. These are in a similar range to those observed in the free ligands, which also exhibit split bands between 1286 and 1219 cm^{-1} and to other reported cyclotetraphosphazenes.[27]

X-ray Crystallographic Studies. $[\{L^1(CuCl_2)_2\}_n]$. The 2:1 reaction between $CuCl_2$ and L^1 gave pale blue needles and X-ray diffraction data were obtained that show that the complex is polymeric. The polymeric structure arises from repeating "$L^1(CuCl_2)$" units that are propagated via a "$Cu(\mu\text{-}Cl)_2Cu$" bridge (Figure 1, selected bond lengths and angles are given in Table 2) to form an infinite chain. The complex crystallizes in the space group *Pnnm* giving rise to a phosphazene ring in which all of the phosphorus atoms are symmetry equivalent.

The copper(II) ions lie in a distorted square-based pyramidal environment with a "N_2Cl_3" donor set (τ value[28] = 0.18). The phosphazene acts as a *trans*-spanning bidentate ligand using nitrogen atoms from pyridine groups on non-geminal phosphorus atoms to bind the copper(II) center with a Cu−N distance of 2.023 Å. The Cu−Cl bond lengths in the basal plane are significantly different, with the copper distance to the bridging chloride being longer [2.3300(17) Å] than the distance to the terminal one [2.2697(19) Å]. The axial bridging Cu−Cl distance is the longest at 2.6204(15) Å. A slight distortion toward trigonal-bipyramidal geometry is apparent from the N−Cu−N bond angle of 164.46(19)° with the Cl1−Cu−Cl2 angle being more regular at 175.55(7)°. The angles around the "$Cu(\mu\text{-}Cl)_2Cu$" bridge are nearly orthogonal: the bridging Cl−Cu−Cl angle is 88.33(5)° and Cu−Cl−Cu is 91.67(5)°.

Table 2. Selected Bond Lengths (Å) and Angles (deg) for $[\{L^1(CuCl_2)_2\}_n]$[a]

Cu1−N11	2.023(3)	Cu1−Cl2	2.3300(17)
Cu1−Cl1	2.2697(19)	Cu1−Cl2(#2)	2.6204(15)
N1−P1	1.562(2)	N1−P2	1.573(2)
N11−Cu1−N11(#1)	164.46(19)	Cl1−Cu1−Cl2	175.55(7)
N11−Cu1−Cl1	89.30(10)	Cl1−Cu1−Cl2(#2)	96.12(6)
N11−Cu1−Cl2(#2)	97.77(9)	Cl2−Cu1−Cl2(#2)	88.33(5)
N11−Cu1−Cl2	90.10(10)	Cu1−Cl2−Cu1(#2)	91.67(5)
N1−P1−N2	120.9(2)		
P1(#1)−N1-P1	137.3(2)	P1(#3)−N1-P1	127.9(3)

[a] Symmetry transformations used to generate equivalent atoms: (#1) *x*, *y*, −*z*; (#2) −*x* + 2, −*y*, −*z*; (#3) −*x* + 1, −*y*, *z*.

The symmetry present in the phosphazene ring means that the phosphorus atoms, N2 and its symmetry equivalent lie in the same plane while N1 and the symmetry equivalent N lie 0.5381 Å above and below this plane. All N−P−N angles are equal at 120.9(2)° while there are two P−N−P angles of 127.9(3) and 137.3(3)°, the larger one being part of the ten-membered chelate ring. These angles and the P−N bond lengths of 1.562(2) and 1.573(2) Å are in the typical ranges for tetrameric cyclophosphazenes.

The "Cu_2Cl_4" core of this structure resembles that in the $[\{Cu(2\text{-}MePy)_2Cl_2\}_2]$ (2-MePy = 2-methylpyridine) dimer,[29] where the formation of a coordination polymer via continuous "$Cu(\mu\text{-}Cl)_2Cu$" bridges (seen in other monodentate *bis*-pyridine derivatives) is not favored, possibly because of the steric bulk of the methyl groups. The Cu−Cu separation in $[\{L^1(CuCl_2)_2\}_n]$ is 3.557 Å and significantly less than in $[\{Cu(2\text{-}MePy)_2Cl_2\}_2]$ (4.404 Å), which is possibly due to the nearly coplanar arrangement of the coordinated pyridine ligands. This is a consequence of the geometry required by the chelate ring and allows a close approach of the otherwise bulky phosphazene ligands. In the monodentate system the pyridine ligands are free to rotate at the Cu−N bond, creating a greater steric effect.

$[L^2(CuCl_2)_2]$. In contrast to the reaction with L^1, the 2:1 reaction between $CuCl_2$ and L^2 and subsequent crystallization produces the discrete, centrosymmetric dimetallic complex, $[L^2(CuCl_2)_2]$ (Figure 2, selected bond lengths and angles are given in Table 3). The copper coordination sphere contains a "N_2Cl_2" donor set with the nitrogen donors N11 and N41A, nitrogen atoms from *cis* non-geminal pyridinoxy rings

(27) Narayanaswamy, P. Y.; Dhathathreyan, K. S.; Krishnamurphy, S. S. *Inorg. Chem.* **1985**, *24*, 640–642.

(28) Addison, A. W.; Rao, T. N.; Reedijk, J.; Van Rijn, J.; Verschoor, G. C. *J. Chem. Soc., Dalton Trans.* **1984**, 1349–1356.

(29) Marsh, W. E.; Hatfield, W. E.; Hodgson, D. J. *Inorg. Chem.* **1982**, *21*, 2679–2684.

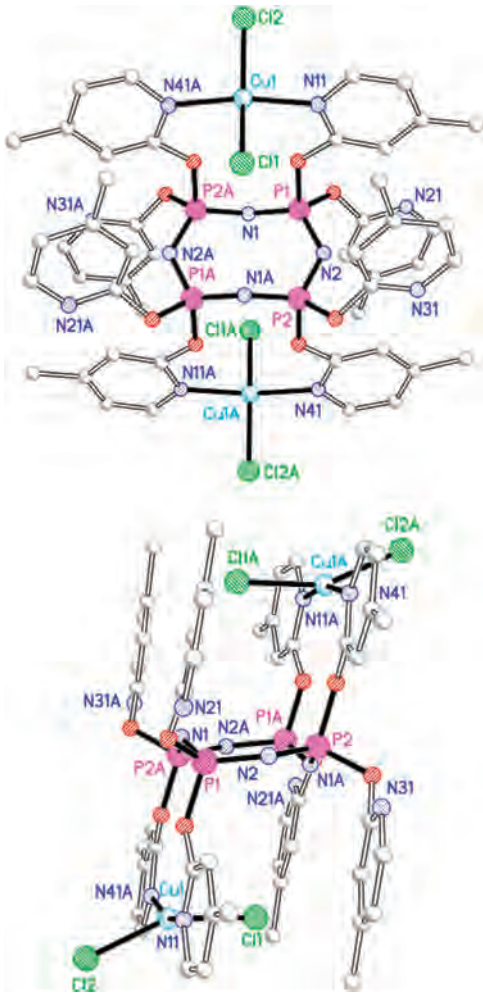

Figure 2. Two views of the complex $[L^2(CuCl_2)_2]$ with the hydrogen atoms removed for clarity.

Table 3. Selected Bond Lengths (Å) and Angles (deg) for $[L^2(CuCl_2)_2]^a$

Cu1−N11	1.9990(18)	Cu1−Cl1	2.2425(6)
Cu1−N41(#1)	2.0057(18)	Cu1−Cl2	2.2351(6)
P1−N1	1.5615(18)	P2−N1(#1)	1.5653(18)
P1−N2	1.5693(19)	P2−N2	1.5701(19)
N11−Cu1−Cl2	92.25(5)	N41(#1)−Cu1−Cl1	91.91(5)
N41(#1)−Cu1−Cl2	92.87(5)	N11−Cu1−N41(#1)	164.37(7)
N11−Cu1−Cl1	89.80(6)	Cl1−Cu1−Cl2	154.50(3)
N1−P1−N2	120.96(10)	P1−N2−P2	128.84(12)
N1(#1)−P2−N2	120.63(10)	P1−N1−P2(#1)	136.62(12)

[a] Symmetry transformation used to generate equivalent atoms: (#1) $-x+1, -y+1, -z$.

coordinating in a similar fashion to $[\{L^1(CuCl_2)_2\}_n]$. Here the equivalent copper(II) ions lie in distorted square planar geometries with the interligand angles in the plane lying between 89.80(6) and 92.25(5)°. Distortion toward tetrahedral geometry is apparent from the N−Cu−N angle of 164.37(7)° and Cl−Cu−Cl angle of 154.50(3)°. The Cu−N bond lengths are 2.0057(18) and 1.990(18) Å, and the Cu−Cl bond lengths are 2.2351(6) and 2.2425(6) Å.

The phosphazene ring has a similar chair conformation to that found in $[\{L^1(CuCl_2)_2\}_n]$ with P1, P2, N2, and their symmetry equivalents, being virtually coplanar and N1, and its symmetry equivalent, lying 0.5451 Å above and below

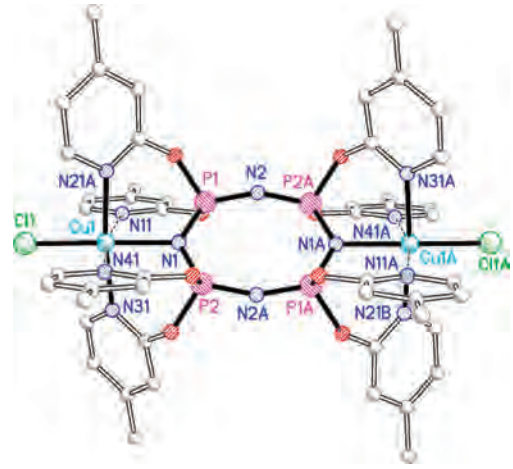

Figure 3. $[L^2(CuCl)_2]^{2+}$ dication showing only one orientation in the disordered pyridine ring system (ring 2) and with hydrogen atoms removed for clarity. Note: the phosphazene ring is positioned in the *XZ* plane for the DFT calculations (cf. Figure 9).

Table 4. Selected Bond Lengths (Å) and Angles (deg) for $[L^2(CuCl)_2](PF_6)_2^a$

Cu1−N1	2.046(2)	Cu1−Cl1	2.2464(7)
Cu1−N11	2.546(3)	Cu1−N31	2.043(2)
Cu1−N21	2.050(2)	Cu1−N41	2.529(3)
N1−P1	1.595(2)	N2−P2(#2)	1.541(2)
N1−P2	1.591(2)	N2−P1	1.543(2)
N1−Cu1−N31	86.69(9)	N31−Cu1−N41	93.01(9)
N31−Cu1−N21	173.13(9)	N1−Cu1−N41	84.27(9)
N1−Cu1−N21	87.18(9)	N21−Cu1−N41	89.48(9)
N21−Cu1−Cl1	93.36(7)	Cl1−Cu1−N41	95.34(6)
N31−Cu1−N11	87.91(9)	N1−Cu1−N11	84.76(9)
N31−Cu1−N21	173.13(9)	N1−Cu1−Cl1	179.33(7)
N41−Cu1−N11	168.92(8)		
P1−N1−P2	128.23(15)	N1−P1−N2	116.49(13)
P2(#2)−N2-P1	150.22(17)	N1−P2−N2(#2)	117.09(13)

[a] Symmetry transformations used to generate equivalent atoms: (#2) $-x+2, -y+2, -z+2$.

the plane. The N−P−N angles in the ring are 120.96(10) and 120.63(10)° and similar to those in the free ligand. However, the pair of P−N−P angles that are involved in forming the chelate rings are less obtuse [128.84(12)°] than the other pair [136.62(12)°] and those in the free ligand [134.09(9) and 146.01(10)°].

$[L^2(CuCl)_2](PF_6)_2$. When $[L^2(CuCl_2)_2]$ is treated with two molar equivalents of $[Ag(MeCN)_4]PF_6$, two chloride ions are abstracted and X-ray quality crystals of the complex $[L^2(CuCl)_2](PF_6)_2$ are obtained from the vapor diffusion of Et_2O into a MeCN solution of the complex. The new centrosymmetric complex contains two six-coordinate Cu(II) centers with "N_5Cl" donor sets, in which the nitrogen donors for each copper are provided by four pyridyl arms and a phosphazene ring nitrogen (Figure 3, selected bond lengths and angles are given in Table 4). In this mode the ligand is behaving as a κ^5 *bis*-tetrapodal bridging ligand. The geometry about the copper is best described as elongated rhombic octahedral containing two short *trans* $Cu-N_{pyridine}$ bonds, Cu1−N21 and Cu1−N31 [2.050(2) and 2.043(2) Å], and two long *trans* $Cu-N_{pyridine}$ bonds, Cu1−N41 and Cu1−N11 [2.529(3) and 2.546(3) Å]. The $Cu-N_{phosphazene}$ bond length is 2.046(2) Å and *trans* to Cu−Cl1 [2.2464 Å]. The

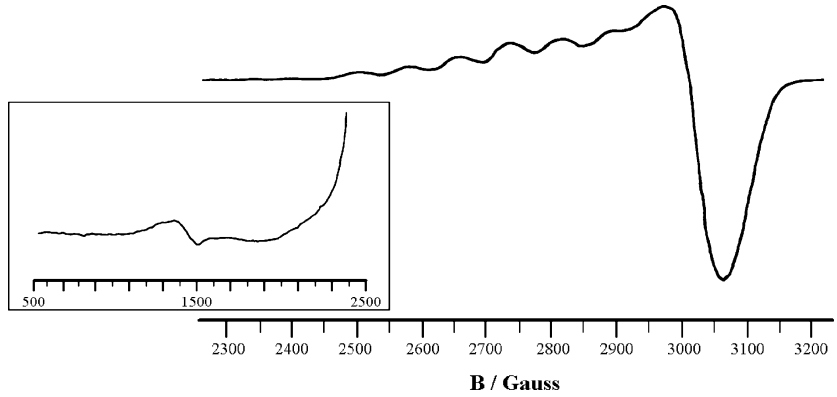

Figure 4. X-band EPR spectrum of $[L^2(CuCl)_2](PF_6)_2$ in frozen nitromethane.

environment is similar to that seen in $[L^3CuCl]PF_6$ although in this complex the $Cu-N_{phosphazene}$ bond length [1.993(3) Å] and the Cu−N bonds on the elongated axis [2.482(3) and 2.467(3) Å] are significantly shorter.[4b]

Coordination of the copper ions to the phosphazene ring in this manner does cause some changes to the ring geometries compared with $[L^2(CuCl_2)_2]$. The ring maintains a chair conformation with the atoms P1, N1, P2, and their symmetry equivalents, being nearly coplanar. N2 and N2A lie 0.3391 Å above and below this mean plane while the copper atoms are 0.0235 Å above and below the plane. In $[L^2(CuCl_2)_2]$ the P−N bond lengths in the ring are all similar (average 1.57 Å) whereas in the $[L^2(CuCl)_2]^{2+}$ dication there are two pairs of long P−N bonds that flank the coordinated ring nitrogens [1.591(2) and 1.595(2) Å] and two pairs of shorter bonds [1.541(2) and 1.543 Å] between the coordinating moieties. The N−P−N bond angles do not change greatly, and the pair of P−N−P bonds involved in the chelate rings are 128.84(12)° and similar to those in $[L^2(CuCl_2)_2]$. However, the second pair of P−N−P bonds are significantly different at 150.22(17)°, and the overall result is that the phosphazene ring in $[L^2(CuCl)_2]^{2+}$ is flattened and more oval-shaped.

It is worth comparing the coordination chemistry of L^1 and L^2 with the cyclotriphosphazene analogues, L^3 and L^4. We reported previously[5] that the reactions of L^3 and L^4 with 2 equiv of copper(II) chloride resulted in the crystallization of markedly different species. In the case of L^3, a trimetallic complex is formed where two $[L^3CuCl]^{2+}$ moieties are linked by a "$CuCl_2$" bridge. In the case of L^4, a neutral dimetallic complex is formed in which L^4 acts as a bridging ligand. The difference in coordination preference is not obvious, although favorable crystal packing forces could play the decisive role. Similarly in the complexes of L^1 and L^2 described here, the origin of the preference for the formation of a coordination polymer over discrete dimetallic units is unclear; the methyl groups in $[L^2(CuCl_2)_2]$ do not seem to encroach the Cu coordination sphere in a manner that would prohibit Cu−Cl bridge formation. Hence, packing forces may again be significant. In both the trimeric and tetrameric systems the presence of more than one species in solution highlights the flexibility of these systems.

However, a difference between the cyclotriphosphazene and cyclotetraphosphazene ligands is apparent in their preferences for binding to the phosphazene ring nitrogen atoms. Ligands L^3 and L^4 all readily form Cu−N bonds to the cyclotriphosphazene ring[4b] whereas the $Cu-N_{phosphazene}$ bond is observed for L^2 only after the treatment of $[L^2(CuCl_2)_2]$ with $[Ag(MeCN)_4]PF_6$ (and here the use of four pyridine rings in the copper coordination sphere of the resulting complex necessarily brings the copper(II) ion close to the phosphazene ring). We have also noticed an absence of ring nitrogen binding in complexes of L^1 and L^2 with Ag(I),[30] and this trend may be of significance when considering a metal binding model for similar ligand substituents on the phosphazene polymer. Cyclotetraphosphazene ring nitrogen coordination by metal ions has been reported before in tungsten and platinum dichoride complexes, although in these cases the tetramers were substituted with electron-releasing amine groups.[15−18] It would appear that the small difference in ring nitrogen basicity between tetramer and trimer [See ref 31a; however, it should be noted that the separation of $N_3P_3Cl_6$ from $N_4P_4Cl_8$ is achieved by the selective protonation of the trimer by sulfuric acid (ref 31b).] becomes more important in deciding whether ring nitrogen metal binding occurs when less electron releasing substituents are present.

Physicochemical Measurements. $[L^2(CuCl)_2](PF_6)_2$. In nitromethane solution, the electronic spectrum of the dimetallic complex, $[L^2(CuCl)_2](PF_6)_2$, displays a broad d-d band at 690 nm ($\varepsilon = 80$ L mol^{-1} cm^{-1} per copper) consistent with the distorted octahedral "N_5Cl" donor set for each of the copper ions and in keeping with its single crystal X-ray structure discussed above. A 10^{-3} M solution of this compound in the same solvent has a conductivity of 147 S cm^2 mol^{-1}, which is typical of a 2:1 electrolyte[32] thus implying the coordinated chloride ions are not ionized and the complex retains its integrity in this solvent. In frozen nitromethane, the X-band EPR spectrum of the complex $[L^2(CuCl)_2](PF_6)_2$ displays well resolved resonances with $g_{||} = 2.31$ and $g_{\perp} = 2.07$ and a weak $g \sim 4.5$ signal (Figure 4). For the $g_{||}$ signal, at least six copper hyperfine lines (average splitting $\sim$ 75 mT) are observed, which is about

(30) Ainscough, E. W.; Brodie, A. M.; Davidson, R. J.; Otter, C. A., unpublished results.
(31) (a) Feakins, D.; Last, W. A.; Neemuchwala, N.; Shaw, R. A. *Chem. Ind.* **1963**, 164–165. (b) Lund, L. G.; Paddock, N. L.; Proctor, J. E.; Searle, H. T. *J. Chem. Soc.* **1960**, 2540–2547.
(32) Geary, W. J. *Coord. Chem. Rev.* **1971**, *7*, 81–122.

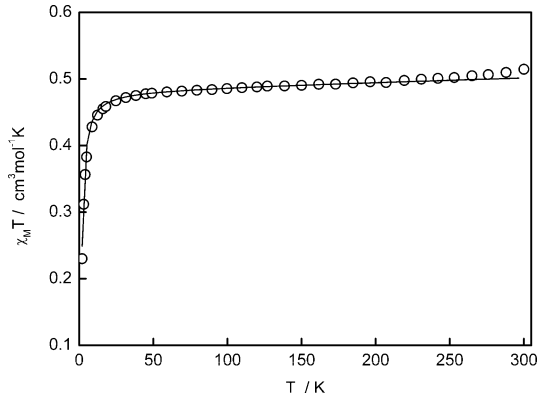

Figure 5. Temperature dependence for $\chi_M T$ (○) for $[L^2(CuCl)_2](PF_6)_2$. The solid line is that calculated using the parameters given in the text.

half that expected for an analogous monomeric complex. These resonances are typical for dimetallic copper(II) complexes where the intradimer exchange parameter *J* is low. As seen in other similar systems,[33−36] the spin forbidden transition ($\Delta M_s = \pm 2$ at $g \sim 4.3$) is only weakly observed, compared to the spin allowed transition ($\Delta M_s = \pm 1$) in the $g = 2$ region. To further probe the coupling of the electron spins on the copper atoms, the variable temperature magnetic susceptibility of the complex has been recorded. The $\chi_M T$ value at 300 K is 0.515 $cm^3\ mol^{-1}$ K ($\mu_{eff} = 2.03\ \mu_B$), close to the values commonly observed for uncoupled Cu(II) compounds. However, the $\chi_M T$ values decrease rapidly as the temperature approaches 0 K (at 2 K the $\chi_M T$ value is 0.228 $cm^3\ mol^{-1}$ K) although an expected Néel temperature maxima was not observed indicating it must be very low (Figure 5). The data were fitted by the Bleaney−Bowers expression for a spin coupled $S_2 = S_2 = {}^1/_2$ system with best-fit parameters of $g = 2.27$ and $2J = -2\ cm^{-1}$ (using a 1% monomeric impurity in the fit). The low value of 2*J* suggests a very weak antiferromagnetic exchange between the Cu(II) centers,[36] but whether the coupling can be rationalized via cyclotetraphosphazene molecular orbitals or via a through space (dipolar) mechanism [the closest Cu····Cu separations are 8.462 Å (intramolecular) and 7.139 Å (intermolecular)] requires a theoretical insight. The DFT calculations (see below) favor coupling via the superexchange pathway provided by the cyclotetraphosphazene p orbitals.

$[L(CuX_2)_2]$ ($L = L^1$, X = Br; $L = L^2$, X = Cl or Br) and $[\{L^1(CuCl_2)_2\}_n]$. The $\chi_M T$ values of the L^1 and L^2 copper(II) halide complexes at 300 K are about 0.405 $cm^3\ mol^{-1}$ K ($\mu_{eff} = 1.80\ \mu_B$) consistent with the normal uncoupled value for copper(II) (Table 5) and, with the exception of $[\{L^1(CuCl_2)_2\}_n]$, show Curie-like susceptibilities with μ_{eff} being independent of temperature. In contrast, the susceptibility versus temperature plot for the latter complex exhibits a Néel temperature maximum at about 12 K, and the corresponding $\chi_M T$ values decrease rapidly below ∼50 K. Again, the data give a good fit to the dimer Bleaney−Bowers expression for a spin coupled system with best-fit parameters of $g = 2.05$ and $2J = -12\ cm^{-1}$ (using a 9% monomeric impurity in the fit, Figure 6). The low value of 2*J* is in line with a weak antiferromagnetic exchange interaction via the bridging chloro atoms. As noted above, the 2-methylpyridine complex, $[\{Cu(2\text{-}MePy)_2Cl_2\}_2]$, is also a chloro-bridged, parallel-planar complex with a comparable 2*J* value of $-7\ cm^{-1}$. Extended Hückel molecular orbital calculations on this and other similar copper(II) systems suggest that the angle at the chloro bridge is the most important factor in determining the sign of the coupling constant, *J*, but the longer out-of-plane Cu−Cl bond distances are significant factors in determining its magnitude.[29] The Cu−Cl−Cu angle is 91.67(5)° for $[\{L^1(CuCl_2)_2\}_n]$ while, for example, in $[\{Cu(2\text{-}MePy)_2Cl_2\}_2]$, it is 100.63(3)° and each has a negative exchange-coupling constant. For $[\{L^1(CuCl_2)_2\}_n]$ the axial bridging Cu−Cl distance is 2.6204(15) Å whereas in $[\{Cu(2\text{-}MePy)_2Cl_2\}_2]$ the corresponding distance is 3.364(1) Å.

The room temperature X-band EPR spectra of polycrystalline powders of the copper halide complexes (Table 5) show broad poorly resolved bands without any observable hyperfine splitting. In frozen nitromethane solution, the spectra are better resolved, and all are typical of monomeric axial copper(II) complexes with $d_{x^2-y^2}$ ground states with $g_{\|} > g_{\perp}$ ($g_{\|} \sim 2.4$, $g_{\|} \sim 2.1$, and $A_{\|} \sim 130 \times 10^{-4}\ cm^{-1}$) which for the polymeric complex $[\{L^1(CuCl_2)_2\}_n]$ implies that it has dissociated into a $[L^1(CuCl_2)_2]$ dimetallic entity with a structure analogous to that found by X-ray crystallography for $[L^2(CuCl_2)_2]$. In comparison with the solid-state spectra, the $g_{\|}$ values have increased and these, along with the $A_{\|}$ values, point to tetrahedrally distorted environments for the copper(II) centers as found for $[L^2(CuCl_2)_2]$ in the solid state. In particular, the $g_{\|}/A_{\|}$ ratios at ∼ 180 cm are above the range expected (105−135 cm) for square planar complexes.[37−39] For example, the "CuN_2Cl_2" square-planar complex $[CuCl_2(diazepam)_2]$ has $g_{\|} = 2.23$ and $A_{\|} = 185 \times 10^{-4}\ cm^{-1}$ which gives a $g_{\|}/A_{\|}$ ratio of 121 cm.[40] Other weaker peaks were observed in these frozen solution spectra implying the presence of minor species in lower concentration.

The electronic spectra of the copper halide complexes (Table 5) display a broad d-d band in the range 590−650 nm, as nujol mulls, characteristic of a tetrahedral distortion of the square-planar arrangement of the "N_2X_2" donor set, as determined in the single crystal X-ray structure of $[L^2(CuCl_2)_2]$ discussed above, and a distorted square-based pyramidal structure with a "N_2Cl_3" donor set with one long axial bridging Cu−Cl distance for $[\{L^1(CuCl_2)_2\}_n]$. Also the bromo complexes have a band at shorter wavelengths assigned to a Br → Cu LMCT.

In nitromethane solution at room temperature, the above light-blue chloro complexes turned light yellow in color, while the bromo analogues are light green and new Cl →

(33) Smith, T. D.; Pilbrow, J. R. *Coord. Chem. Rev.* **1974**, *13*, 173–278.
(34) Addison, A. W.; Burke, P. J.; Henrick, K. *Inorg. Chem.* **1982**, *21*, 60–63.
(35) Pierpont, C. G.; Francesconi, L. C.; Hendrickson, D. N. *Inorg. Chem.* **1978**, *17*, 3470–3477.
(36) Klingele, J.; Moubaraki, B.; Murray, K. S.; Boas, J. F.; Brooker, S. *Eur. J. Inorg. Chem.* **2005**, 1530–1541.
(37) Sakaguchi, U.; Addison, A. W. *J. Chem. Soc., Dalton Trans.* **1979**, 600–608.
(38) Yokoi, H.; Addison, A. W. *Inorg. Chem.* **1977**, *16*, 1341–1349.
(39) Niklas, N.; Alsfasser, R. *Dalton Trans.* **2006**, 3188–3199.
(40) Mosset, A.; Tuchagues, J. P.; Bonnett, J. J.; Haran, R.; Sharrock, P. *Inorg. Chem.* **1980**, *19*, 290–294.

Table 5. Electronic Spectral, Magnetic and EPR Spectral Data for the Complexes

compound	electronic spectral data/nm		magnetic moments/μ_B	EPR spectral data				
				solid state[c]		frozen solution[d]		
	solution[a]	solid[b]		$g_{\|\|}$	$g\perp$	$g_{\|\|}$	$g\perp$	$A_{\|\|}$/cm^{-1}
$[\{L^1(CuCl_2)_2\}_n]$	463[e], 765 (100)	650	1.83	2.26 br	2.07	2.43	2.07	130×10^{-4}
$[L^2(CuCl_2)_2]$	464[e], 680 (50), 795 (35)	590	1.82	2.27 br	2.07	2.43	2.09	136×10^{-4}
$[L^1(CuBr_2)_2]$	420sh[e], 644,[e] 870 (115)	415[e], 645	1.86	2.22	2.08	2.42	2.09	138×10^{-4}
$[L^2(CuBr_2)_2]$	648[e,f]	420[e], 620	1.79	2.26 br	2.12 br	2.42	2.09 br	133×10^{-4}
$[L^2(CuCl)_2](PF_6)_2$	690 (80)		2.03	2.27 br	2.07	2.31	2.07[g]	81×10^{-4}

[a] In CH_3NO_2, molar absorption coefficients (L mol^{-1} cm^{-1}) calculated per Cu given in parentheses. [b] As nujol mulls. [c] Room temperature. [d] At 110 K in CH_3NO_2. [e] Assigned to X → Cu(II) CT band. [f] CT absorption at 648 nm obscures the d-d band. [g] A weak $\Delta M_s = \pm 2$ transition observed at $g \sim 4.5$.

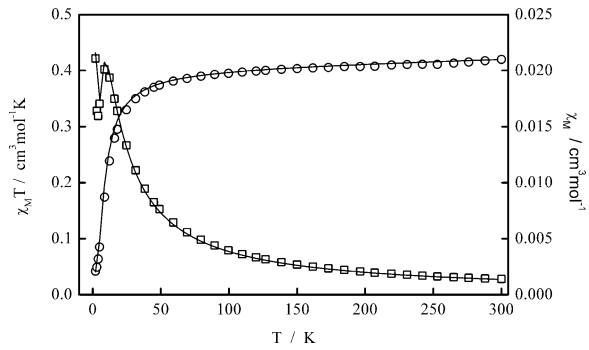

Figure 6. Temperature dependence for $\chi_M T$ (○) and molar susceptibilities χ_M (□) for $[\{L^1(CuCl_2)_2\}_n]$. The solid lines are those calculated using the parameters given in the text.

Cu and Br → Cu LMCT bands are observed at about 460 and 645 nm, indicative of the presence of the $[Cu_2Cl_6]^{2-}$ and $[Cu_2Br_6]^{2-}$ ions, respectively.[4a,41] This suggests a partial dissociation of the complexes as illustrated by the representative equation for L^1:

$$2[L^1(CuCl_2)_2] \rightarrow 2[L^1(CuCl)]^+ + [Cu_2Cl_6]^{2-} \qquad (1)$$

From the CT band at 460 nm for the pure $[Cu_2Cl_6]^{2-}$ ion, it is possible to determine that ~70% of the complex has rearranged according to the equation above, while for the analogous system containing the L^2 ligand only about 13% has rearranged. The formation of ionic species is supported by molar conductivities that range from 95 to 130 S cm^2 mol^{-1} for 10^{-3} M nitromethane solutions.

DFT Calculations. To rationalize the observed weak antiferromagnetic coupling observed in the ESR and magnetic measurements of $[L^2(CuCl)_2](PF_6)_2$, a computational study was performed on the dication $[L^2(CuCl)_2]^{2+}$. For comparison, a calculation has also been carried out on the related cyclotriphosphazene complex, $[L^4(CuCl_2)_2]$, which contains two symmetry-related five coordinated copper(II) ions in a square-based pyramidal-distorted trigonal-bipyramidal environment (Chart 2). In this complex, the copper ions, which are 6.472 Å apart, are also weakly antiferromagnetically coupled with $2J = -1$ cm^{-1} and a hyperfine splitting in the $g_{||}$ region of ~ 60 mT of the EPR spectrum as a result of weak coupling between the copper centers.[4b]

Analysis of all occupied molecular orbitals involving the copper ions, revealed a pair of orbitals in each complex that could explain the weak antiferromagnetic coupling (Figures 7 and 8). In the cyclotetraphosphazene complex, $[L^2(CuCl)_2]^{2+}$, this is made up of contributions from out-of-plane nitrogen p_y orbitals interacting with the metal ions and the uncoordinated in-plane nitrogen p_z orbitals (Figure 9). The calculations show the separation between the low and high energy orbitals is small (0.024 eV). However, the low energy orbital (Figure 9a) does provide an "electron-density-bridge" linking the copper(II) centers, and would provide a mechanism for the very weak antiferromagnetic coupling observed in the complex. An examination of the atomic orbital coefficients (Table S1, Supporting Information) shows that the orbital consists primarily of the p_z and p_y nitrogen orbitals and the d_{xy} orbitals of the metal ions with a negligible contribution from the phosphorus atom orbitals (Figure 9b). A similar "electron-density-bridge" orbital (Figure 10a) which links the two copper centers is also found in the cyclotriphosphazene complex, $[L^4(CuCl_2)_2]$. As with $[L^2(CuCl)_2]^{2+}$, the phosphazene ring contribution to this orbital consists of the in-plane p_y and out-of-plane p_z orbitals of the phosphazene ring nitrogens atoms with negligible contribution from the phosphorus atoms (Table S2, Supporting Information). However, since the copper ions are held 28° out of the phosphazene ring, rather than being coplanar with it as for $[L^2(CuCl)_2]^{2+}$, the copper orbitals are mainly $d_{x^2-y^2}$ in character, not d_{xy} (Figure 10b).

The observation of "electron-density-bridge" orbitals with contributions from phosphazene nitrogen p orbitals is consistent with the ionic contribution of the P−N bonding being the dominant component within the phosphazene rings (not negative hyperconjugation which is the "aromatic" component) since it is the ring nitrogen atoms that are negatively charged. Hence for $[L^2(CuCl)_2]^{2+}$, the formation of an "electron-density-bridge" can be rationalized by the two positively charged copper ions causing an expansion of the electron density of the in-plane p_z-type orbitals of the uncoordinated nitrogen atoms thus allowing them to overlap with the coordinated nitrogen p_y orbitals (Figure 9). The magnitude of the antiferromagnetic coupling between the copper(II) centers that occurs via the phosphazene ring systems is similar to that observed in dinuclear copper(II) complexes of pyrazine-based ligands. For example, a $2J$ value of -0.48 cm^{-1} is exhibited by $[Cu_2L(MeCN)_2(H_2O)_2](BF_4)_2$ [H_2L = *N,N′*-bis(2-pyridylmethyl)pyrazine-2,5-dicarboxamide] although the Cu····Cu coupling is via the aromatic $2p_\pi$ system.[36] The magnitude of the coupling does not appear to be markedly influenced by the Cu····Cu distance, which at 6.811 Å in the pyrazine ligand complex is shorter than the analogous distance of 8.462 Å found in

(41) Scott, B.; Willett, R. D. *J. Am. Chem. Soc.* **1991**, *113*, 5253–5258.

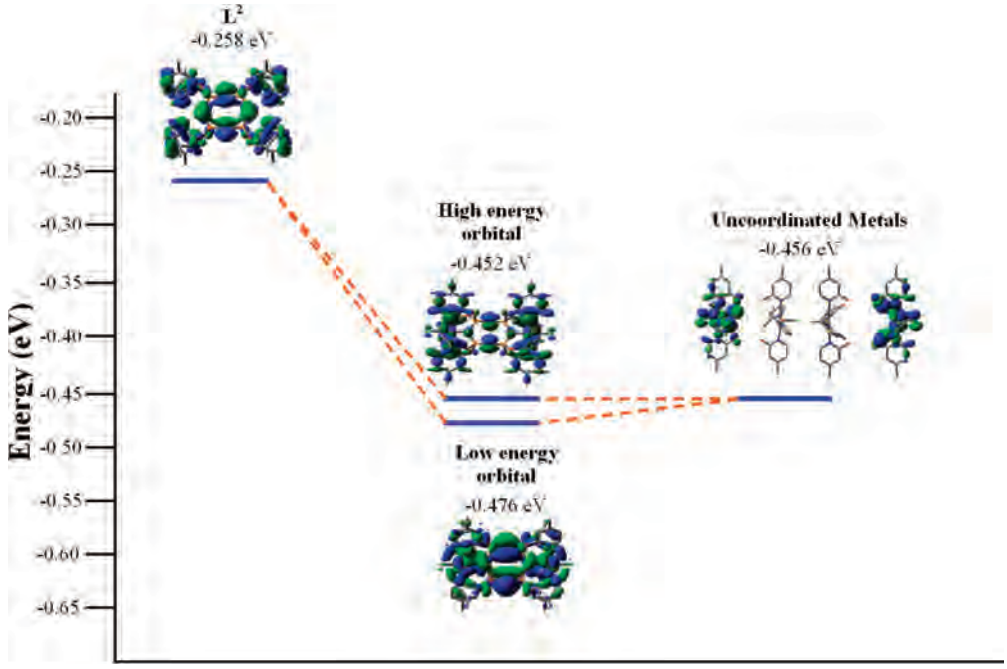

Figure 7. Energy level diagram for the "electron-density-bridge" molecular orbitals for $[L^2(CuCl)_2]^{2+}$.

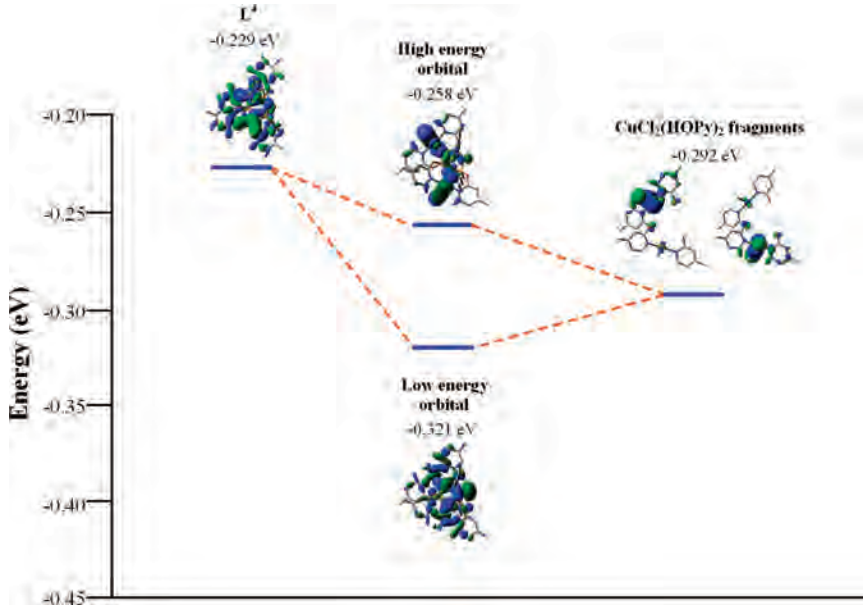

Figure 8. Energy level diagram for the "electron-density-bridge" molecular orbitals for $[L^4(CuCl_2)_2]$.

the tetrameric phosphazene complex, $[L^2(CuCl)_2](PF_6)_2$ but similar to that (6.472 Å) in the trimeric complex, $[L^4(CuCl_2)_2]$.

Conclusion

The ligands, octakis(2-pyridyloxy)cyclotetraphosphazene (L^1) and octakis(4-methyl-2-pyridylxy)cyclotetraphosphazene (L^2), form 2:1 products with copper(II) chloride or bromide when 1 or 2 equiv of the metal salt are used. Three different structural types, as illustrated by $[\{L^1(CuCl_2)_2\}_n]$, $[L^2(CuCl_2)_2]$, and $[L^2(CuCl)_2](PF_6)_2$, have been identified and their structures characterized by X-ray crystallography. The complex, $[\{L^1(CuCl_2)_2\}_n]$, is a coordination polymer propagated by interligand "Cu(μ-Cl)$_2$Cu" bridges whereas $[L^2(CuCl_2)_2]$ forms discrete dimetallic cyclotetraphosphazene-based moieties. The variable temperature magnetic susceptibility data for $[\{L^1(CuCl_2)_2\}_n]$ are consistent with a weak antiferromagnetic exchange interaction between the copper(II) centers occurring via the bridging chloro atoms. In contrast, $[L^2(CuCl_2)_2]$ and the dicopper(II) bromide complexes, $[L(CuBr_2)_2]$ ($L = L^1$ and L^2), exhibit normal Curie-like susceptibilities with μ_{eff} being independent of temperature. When $[Ag(MeCN)_4](PF_6)$ abstracts a chloride ion from each copper site in $[L^2(CuCl_2)_2]$, two of the free pyridine ring nitrogen donors swing in to bind to the metal thus encouraging a phosphazene ring nitrogen to also bind as $[L^2(CuCl)_2](PF_6)_2$ is formed. In this complex, the copper(II) ions are separated by "N—P═N—P═N" phosphazene bridges

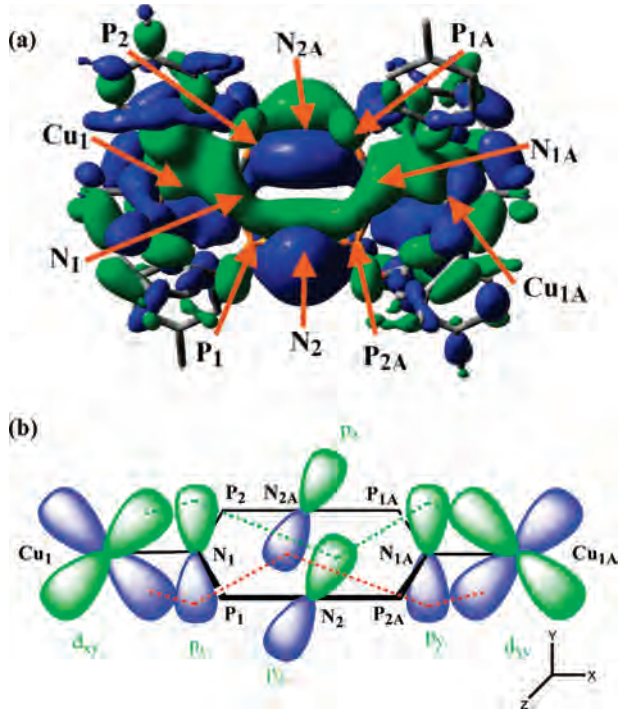

Figure 9. (a) HOMO -35β (HOMO -8β with respect to the phosphazene ring) in $[L^2(CuCl)_2]^{2+}$ showing the "electron-density-bridge" (orbital isosurface exaggerated for clarity) linking the copper(II) ions and (b) schematic view of the "electron-density-bridge".

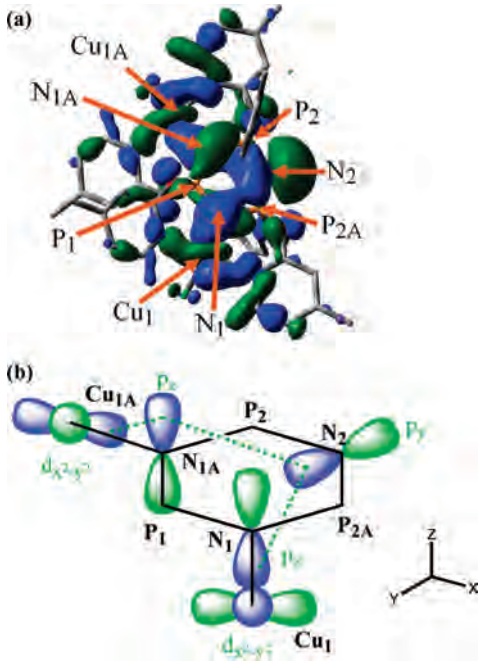

Figure 10. (a) HOMO -34β (HOMO -7β with respect to the phosphazene ring) in $[L^4(CuCl_2)_2]$ showing the "electron-density-bridge" (orbital isosurface exaggerated for clarity) linking the copper(II) ions and (b) schematic view of the "electron-density-bridge".

which allows weak antiferromagnetic coupling of the unpaired electrons on the copper(II) centers. From DFT calculations on the dication, $[L^2(CuCl)_2]^{2+}$, and the cyclotriphosphazene dicopper complex, $[L^4(CuCl_2)_2]$, "electron-density-bridge" molecular orbitals which involve Cu 3d orbitals overlapping with the non-bonding N-based molecular orbitals on the phosphazene rings have been identified as the pathway for this interaction. The observation that the electronic communication between the copper(II) centers is weak is consistent with the electrochemical results on the di-iron compound, $[(FeI_2)_2\{N_3P_3(pyNH)_2(MeNC_2H_4NMe)_2\}]$, where only one oxidation corresponding to the Fe^{2+}/Fe^{3+} couple was assigned.[42] Overall these results support recent ab initio calculations on phosphazenes which emphasize the predominance of the role of the ionic component of bonding in the phosphazene P−N bond, but the negative hyperconjugation component is needed for a complete bonding description.[22] It is not surprising that phosphorus based 3d orbitals are not required to explain the electron delocalization in these complexes, since the ab initio calculations show that they play little role in the bonding scheme in phosphazenes.

The present study provides further evidence that the multiple bond character of phosphazenes is quite different from the π-π interactions found in carbon-based aromatic ring systems. However, it does raise the intriguing possibility that metal−metal communication along the phosphazene backbone in phosphazene polymers may be possible if paramagnetic metal ions are bound directly to the backbone phosphazene nitrogen atoms but separated from each other by not more than one or two P−N units.

Acknowledgment. We acknowledge financial support, including a postdoctoral fellowship (to C.A.O.), from the Massey University Research Fund and the RSNZ Marsden Fund (MAU208). We thank the Otsuka Chemical Co. Ltd. for a gift of octachlorocyclotetraphosphazene. We are also grateful to Dr J. A. Harrison for helpful advice (Massey University, Auckland), Professor P. A. Schwerdtfeger for generous access to the Helix parallel-computing facility (Massey University, Auckland), and to Dr J. L. Wikaira (Canterbury University) and Professor S. A. Brooker (Otago University) for assistance in collecting X-ray crystallographic data.

Supporting Information Available: Crystallographic information for $[\{L^1(CuCl_2)_2\}\cdot 2MeCN\cdot H_2O]_n$, $[L^2(CuCl_2)_2]$ and $[L^2(CuCl)_2](PF_6)_2\cdot 6MeCN$ in CIF format, calculated and experimental bond length data (Figure S1), atomic orbital coefficients for the "electron density bridge" molecular orbital, and optimized geometries for the dimetallic cations, $[L^2(CuCl)_2]^{2+}$ and $[L^4(CuCl)_2]^{2+}$ (Tables S1−S4). This material is available free of charge via the Internet at http://pubs.acs.org.

IC8008706

(42) Harmjanz, M.; Piglosiewicz, I. M.; Scott, B. L.; Burns, C. J. *Inorg. Chem.* **2004**, *43*, 642–650.